VIETNAM JOURNAL OF HYDROMETEOROLOGY

Research Article

Application of GSMaP Satellite data in precipitation estimation and nowcasting: evaluations for October 2019 to January 2020 period for Vietnam

Mai Khanh Hung[1*], Kazuo Saito[2,3,4], Mai Van Khiem[1], Du Duc Tien[1], Nguyen Viet Hung[5]

[1] National Center for Hydro–Meteorological Forecasting; maikhanhhung18988@gmail.com; maikhiem77@gmail.com; duductien@gmail.com
[2] Japan Meteorological Business Support Center, Japan; k–saito@jmbsc.or.jp
[3] Atmosphere and Ocean Research Institute, University of Tokyo, Japan; k_saito@aori.u.tokyo.ac.jp
[4] Meteorological Research Institute, Japan Meteorological Agency, Japan; ksaito@mri–jam.go.jp
[5] Aero Meteorological Observatory; truongphi115@gmail.com
* Correspondence: maikhanhhung18988@gmail.com; Tel.: +84916400000

Received: 05 June 2020; Accepted: 20 August 2020; Published: 25 August 2020

Abstract: The GSMaP Rainfall (Global Satellite Mapping of Precipitation) data (GSMaP_NOW and GSMaP_MVK) have been used for precipitation analysis at Vietnamese National Center for Hydro–Meteorological Forecasting (NCHMF) since October 2019. This study verified the quality of rainfall estimates of GSMaP_NOW, GSMaP _MVK and Himawari–8 based on 6 hourly rain gauge data from 184 SYNOP stations for a 4–month period from October 2019 to January 2020. The results show that GSMaP_MVK has the best rainfall estimate among the three data types in terms of RMSE, correlation and other categorical statistics except the probabilty of detection (POD). GSMaP_NOW was better than Himawari–8 for RMSE, correlation, and flase alarm rate, whilethe threat scores of GSMaP_NOW and Himawari–8 were in the same level. Himawari–8 tended to overestimate intense rains, and its bias scores were very large. This overestimation is significant when the cloud top temperature of prerecipitation system is very low. GSMaP_NOW can be used in parallel with Himawari–8 rainfall estimates to provide realtime information to the forecasters in forecasting and warning on the heavy rainfall, flash flood and landslide.

Keywords: Satellite precipitation estimates; GSMaP_NOW; GSMaP_MVK; Himawari–8; Precipitation nowcasting; Verification of rainall.

1. Introduction

Vietnam is one of the countries that suffers from many natural disasters every year [1]. In particular, disasters by heavy rains often cause the greatest damage in Vietnam. Therefore, monitoring, forecasting and warning of heavy rainfall, flash floods, landslides, and land subsidence due to floods are necessary and also the most important tasks of the Vietnamese National Center for Hydro–Meteorological Forecasting (NCHMF). In the past, forecasters carried out these works mainly based on rain gauge data and radar precipitation estimates. However, the density of observatories and radar stations is sparse. This makes it difficult for forecasters in heavy rainfall monitoring, forecasting and floods and landslides warning,

especially in areas where rainfall observations are limited. Rainfall estimates from satellites have been used to compensate this problem. In the world, there are many studies showing the effectiveness of satellite precipitation estimates in forecasting heavy rainfall landslides and flash floods [2–3].

Currently, NCHMF is receiving satellite Himawari–8 precipitation estimates from Aero Meteorological Observatory (AMO) operationally. These data provide precipitation information for areas where rain gauge observation stations and radar–estimated rainfall are insufficient. Himawari–8 rainfall estimates are used by forecasters to monitor cloud systems and update rainfall level to give timely forecastings and to warn heavy rain, flash flood and landslide. However, there are limitations in Himawari–8 data to accurately estimate precipitation, because it observes cloud systems by the brightness temperature [4–5]. These are difficulties for forecasters in monitoring, forecasting and warning heavy rain. An additional satellite rainfall estimate is needed to continuously provide rainfall information to forecasters. The GSMaP (Global Satellite Mapping of Precipitation) rainfall data is a useful solution. There are many studies proving the role of GSMaP in operational forecasts and research. GSMaP precipitation data is high–resolution estimates of rainfall based on satellite microwave radiometers provided by the Japan Science and Technology Agency (JST) and the Japan Space Exploration Agency (JAXA). GSMaP data have been evaluated and applied in many parts of the world [6–7]. In Vietnam, Ngo Duc Thanh et al. examined performance of GSMaP in central Vietnam for long–term rain [8].

Recently, Saito et al. [5] tested GSMaP data to improve the precipitation analysis at NCHMF. They compared the accuracy of precipitation estimates by GSMaP_NOW, GSMaP_MVK and Himawari–8 against AWS precipitation for a heavy rainfall case in central Vietnam in December 2018. Since October 2019, GSMaP has been used for operation at NCHMF. In order to confirm that GSMaP_NOW and MVK data are suitable for the operation, it is necessary to validate them for a long–term period. Based on that reason, this study carried out the evaluation of GSMaP_NOW and MKV in the period from October 2019 to the end of January 2020 as a foundation for applying this data in business.

2. Materials and Methods

2.1. Framework of Research

The aim of this research is to verify the 6–hour rainfall estimates from Himawari–8, GSMaP_NOW and GSMaP_MVK against rain gauge data. The data series used for this verification is four months from October 2019 to January 2020. Himawari–8 satellite estimates of rainfall are provided hourly from AMO to NCHMF with a horizontal resolution of 5km (0.045 degree). In this study, the 6–hour rainfall amount was calculated as the sum of six consecutive hourly rainfall estimates data. GSMAP_MKV is high–resolution (0.1 degree) global rain estimate with short time steps (1 hour) using passive microwave radiation measurement data by GPM satellites. This data was smoothed out based on the Kalman filter model, which is based on analysis of atmospheric motion vectors obtained from two consecutive infrared images by geostationary satellites [9–10]. JAXA develops a near real–time version of GSMAP products (GSMaP_NRT) for the monitored area of the Himawari–8 to create rainfall estimates in real time. After that, the next 0.5hours data is extrapolated by atmospheric motion vectors to create the GSMAP_NOW rain product at the present time with available satellite microwave data [11–12].

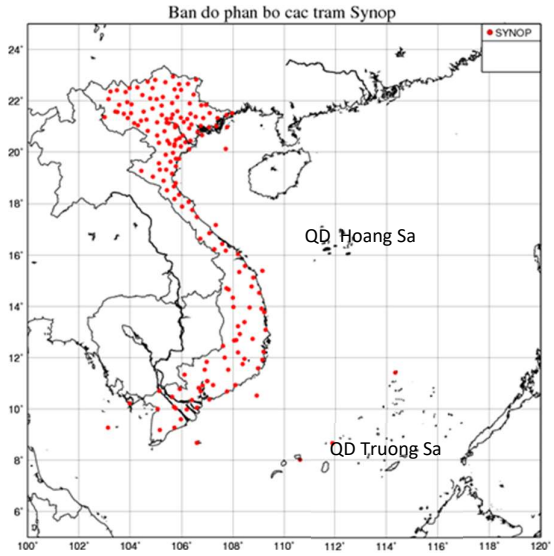

Figure 1. Distribution of 184 SYNOP rain gauges in Vietnam.

Table 1. Detailed GSMaP products.

	Resolution	**Latency**	**Update interval**
MVK	Horizontal: 0.1x0.1 deg.lat/lon Temporal: 01 hour	3 day(s)	01 hour (s)
NOW		0 hour(s)	0.5 hour(s)

There are 184 SYNOP rain gauge stations available in Vietnam and the distribution of rainfall stations is shown in Figure1 and Table 2. Rain gauge data which represent the rainfall at these points were used as reference in comparison of study. The rain gauge data were monitored and evaluated to control the quality processes to eliminate errors. Himawari–8, GSMaP_NOW and GSMaP_MVK grid rainfall estimates data were interpolated to these 184 positions of rain gauge stations. In this study, the nearest neighbor interpolation method was chosen. Due to the high localization rain, the nearest interpolation method reduces the influence of the terrain during interpolation. In this interpolation method, the distances from the positions of rain gauge stations to the grid nodes of the rainfall estimates data are calculated, and the value at the nearest grid point is assigned to the rain gauge point. Note that in Saito et al. (2020) [5], GSMaP and Himawari–8 3–hour rainfall estimates were verified against AWS data with interpolated verification grids of 5 km horizontal resolution.

Table 2. SYNOP rain gauge stations.

Name	**Lat**	**Lon**	**Name**	**Lat**	**Lon**	**Name**	**Lat**	**Lon**	**Name**	**Lat**	**Lon**	**Name**	**Lat**	**Lon**
Muong Te	22.4	102.8	Chiem Hoa	22.2	105.3	Son Tay	21.2	105.5	Ba Don	17.8	106.4	Lak	12.2	108.2
Sin Ho	22.4	103.2	Cho Ra	22.5	105.7	Lang	21	105.8	Con Co	17.2	107.4	Dac Mil	12.5	107.6
am Duong	22.4	103.5	Ngan Son	22.4	105.7	Hoai Duc	21.1	105.8	Dong Ha	16.8	107.1	Dak Nong	12	107.7
Than Uyen	22	103.9	Bac Can	22.2	105	Ha Dong	21	105.8	Khe Sanh	16.6	106.7	Da Lat	12	108.5
Muong Lay	22.1	103.2	Thai Nguyen	21.6	105.8	Chi Linh	21.1	106.4	Hue	16.4	107.6	Lien Khuong	11.7	108.4
Tuan Giao	21.6	103.4	Dinh Hoa	21.9	105.6	Hai Duong	21	106.3	A Luoi	16.2	107.3	Bao Loc	11.5	107.8
Pha Din	21.6	103.5	Minh Dai	21	105.1	Hung Yen	20.7	106.1	Nam Dong	16.2	107.7	Cat Tien	11.6	107.4
Dien Bien	21.4	103	Phu Ho	21.5	105.2	Nam Dinh	20.4	106.2	Da Nang	16.1	108.4	Phuoc Long	11.8	107

Name	Lat	Lon	Name	Lat	Lon	Name	Lat	Lon	Name	Lat	Lon	Name	Lat	Lon
Phieng Lanh	21.9	103.6	Viet Tri	21.3	105.4	Van Ly	20.1	106.3	Tam Ky	15.6	108.5	Dong Phu	11.5	106.9
Muong La	21.9	104.1	Vinh Yen	21.3	105.6	Phu Ly	20.5	105.9	Tra My	15.4	108.2	Tay Ninh	11.3	106.1
Son La	21.3	103.9	Tam Dao	21.5	105.7	Nho Quan	20.3	105.8	Ly Son	15.4	109.2	Tri An	11.1	107
Song Ma	21.1	103.8	Cao Bang	22.7	106.3	Ninh Binh	20.3	106	Q.Ngai	15.1	108.8	Bien Hoa	10.9	106.8
Co Noi	21.1	104.2	Bao Lac	23	105.7	C.Phuong	20.3	105.7	BaTo	14.8	108.7	Ta Lai	11.4	107.4
Yen Chau	21.1	103.3	Nguyen Binh	22.7	106	Thai Binh	20.4	106.4	Hoai Nhon	14.1	109	Long Khanh	10.9	107.2
Bac Yen	21.2	104.4	T.Khanh	22.8	106.5	Hoi Xuan	20.4	105.1	An Nhon	13.9	109.1	Thu Dau Mot	11	106.6
Phu Yen	21.3	104.6	That Khe	22.3	106.5	Yen Dinh	20	105.7	Quy Nhon	13.8	109.2	Nha Be	10.8	106.7
Moc Chau	20.8	104.7	Lang Son	21.8	106.8	SamSon	19.8	105.9	Son Hoa	13.1	109	Vung Tau	10.4	107.1
Mai Chau	20.7	105.1	Mau Son	21.9	107	Bai Thuong	19.9	105.9	Tuy Hoa	13.1	109.3	Con Dao	8.7	106.6
Kim Boi	20.7	105.5	Bac Son	21.9	106.3	Thanh Hoa	19.8	105.8	Nha Trang	12.3	109.1	Huyen Tran	8	110.6
Chi Ne	20.5	105.8	Huu Lung	21.8	106.6	Nhu Xuan	19.6	105.6	Cam Ranh	11.9	109.2	Moc Hoa	10.8	105.9
Lac Son	20.5	105.5	Dinh Lap	21.5	107.1	Tinh Gia	19.5	105.8	SongTTay	11.4	114.3	My Tho	10.4	106.4
Hoa Binh	20.8	105.3	Mong Cai	21.5	108	Quy Chau	19.4	105.1	Phan Rang	11.6	109	Vinh Long	10.3	106
Lao Cai	22.5	104	Quang Ha	21.5	107.8	Tuong Duong	19.3	104.5	Phan Thiet	10.9	108.1	Ben Tre	10.2	106.4
Bac Ha	22.5	104.3	TienYen	21.3	107.4	Quy Hop	19.5	105.3	LaGi	10.7	107.8	Ba Tri	10.1	106.6
SaPa	22.4	103.8	CoTo	21	107.8	Tay Hieu	19.3	105.4	Phu Quy	10.5	108.9	Cao Lanh	8	106.6
Pho Rang	22.2	104.5	CuaOng	21	107.4	Con Cuong	19.1	104.9	Phan Ri	11.2	108.5	Cang Long	10	106.2
Mu.C.Chai	21.9	104.1	BaiChay	21	107.1	Quynh Luu	19.1	105.6	Dak To	14.7	107.8	ChauDoc	10.7	105.1
Yen Bai	21.7	104.4	UongBi	21	106.8	Do Luong	18.8	105.3	Kon Tum	14.4	108	Tra Noc	10.1	105.7
Van Chan	21.6	104.5	HiepHoa	21.4	106	Hon Ngu	18.8	105.8	Playcu	14	108	Can Tho	10	105.8
Luc Yen	22.1	104.7	LucNgan	21.4	106.6	Vinh	18.7	105.7	An Khe	14	108.7	Vi Thanh	9.8	105.5
Ha Giang	22.8	105	SonDong	21.3	106.8	Huong Son	18.9	105.7	Yaly	14.7	107.8	Soc Trang	9.6	106
Hoang SPhi	22.8	104.7	BacGiang	21.3	106.2	Ha Tinh	18.4	105.9	Ayunpa	13.4	108.5	Rach Gia	10	105.1
Bac Me	22.7	105.4	BacNinh	21.2	106.1	Huong Khe	18.2	105.7	EaHleo	13.4	108.3	Phu Quoc	10.2	104
Bac Quang	22.5	104.9	PhuLien	20.8	106.6	Hoanh Son	18	106.5	Buon Ho	12.9	108.3	Tho Chu	9.3	103.5
Dong Van	23.3	105.3	HonDau	20.7	106.8	Ky Anh	18.1	106.3	MDrak	12.7	108.8	Bac Lieu	9.3	105.7
T.Quang	21.8	105.2	Bach.L.Vi	20.1	107.7	Tuyen Hoa	17.9	106	B.MThuot	12.7	108.1	Ca Mau	9.2	105.2
Ham Yen	22.1	105	BaVi	21.2	105.4	Dong Hoi	17.5	106.6	EaKmat	12.7	108.1			

2.2. Verification method

2.2.1. Continuous statistical verifications

The main aim of this method was to measure the correspondence between the estimated rainfall and the observation. To quantify this correspondence value, the following three statistical indices were used the mean error (ME), the root mean square (RMSE) and the correlation coefficient (CORR) [13].

$$ME = \frac{1}{N}\sum_{i=1}^{N}(F_i - O_i) \quad (1)$$

$$RMSE = \sqrt{\frac{1}{N}\sum_{i=1}^{N}(F_i - O_i)^2} \quad (2)$$

$$CORR = \frac{\sum_{i=1}^{N}(F_i - \bar{F})(O_i - \bar{O})}{\sqrt{\frac{1}{N}\sum_{i=1}^{N}(F_i - \bar{F})^2}\sqrt{\frac{1}{N}\sum_{i=1}^{N}(O_i - \bar{O})^2}} \quad (3)$$

where F_i is the satellite estimates, O_i is rain gauge values, $\bar{F}$ is mean of the satellite estimates, $\bar{O}$ is mean of the rain gauge values and *n* is total number of rain gauge (rainfall estimated data).

2.2.2. Categorical statistical verifications

In this study, the correspondence between the estimated and observed occurrence of events is measured by categorical statistics. Table 3 summarizes the contingency to verify satellite rainfall detection capability with rain or no rain events following thresholds from 1mm/6h to 100mm/6h.

Table 3. Contingency table of yes or no events with rain or no rain.

		Observed rainfall	
		Yes	No
Estimated Rainfall	Yes	hits	false alarms
	No	misses	correct negative

In Table 3, "hits" shows correctly estimated rain events, "misses" means when the rain is not estimated but in fact the rain occurs, "false alarm" describes when rain events is estimated but actual rain events do not occur, and "correct negative" correctly shows no rain events occur. Five categorical statistics indices used are the frequency bias (BIAS), probability of detection (POD), the false alarm ratio (FAR), the threat score (TS) and equitable threat score (ETS). BIAS, POD, FAR, TS and ETS indices are calculated as [13]:

$$\text{BIAS} = \frac{\text{hits+false alarm}}{\text{hits+misses}} \quad (4)$$

$$\text{POD} = \frac{\text{hits}}{\text{hits+misses}} \quad (5)$$

$$\text{FAR} = \frac{\text{false alarm}}{\text{hits+false alarm}} \quad (6)$$

$$\text{TS} = \frac{\text{hits}}{\text{hits+misses+false alarm}} \quad (7)$$

$$\text{ETS} = \frac{\text{hits - hits}_{random}}{\text{hits+misses+false alarm-hits}_{random}} \quad (8)$$

$$\text{Where } \text{hits}_{random} = P_c(\text{hits+false alarm}) \quad (9)$$

$$\text{And} \quad P_c = \frac{\text{hits+misses}}{\text{hits+misses} + \text{false alarm+correct negative}} \tag{10}$$

BIAS measures the ratio of the frequency of forecast events to the frequency of observed events. The forecast system tends to underforecast (BIAS<1) or overforecast (BIAS>1) events, and BIAS does not measure how well the forecast corresponds to the observations, but only measures relative frequencies. POD describes how often the estimate detected correctly the occurrence of rain events. Range of POD is from 0 to 1 and perfect score is 1. FAR shows the fraction of diagnosed events that turned out to be wrong. Range of FAR value is from 0 to 1. The perfect score is 0. TS shows how well the estimate implied "yes" events to correspond with the observed "yes" events. It measures the fraction of observed and/or estimated events that were correct. It can be thought of as the accuracy when correct negatives have been removed from consideration, which means that TS is only concerned with estimates that count. Sensitive to hits, penalizes both misses and false alarms. ETS is like TS, but it removes the contribution from hits by chance in the random forecast.

3. Results

3.1. Continuous Statistical verifications

Figures 2–4 are scatter plots which describe the correspondence between the 6–hour rainfall estimates from Himawari–8(HWM), GSMaP_NOW(NOW), GSMaP_MVK(MVK) and the 6–hour rains at SYNOP stations. In these scatter plots, the dashed blue line is the linear regression line between estimated rainfall and observed rainfall. The correlation coefficient (CORR), RMSE and ME values are displayed in the lower right corner. The solid blue diagonal line is the ideal regression or "45–degree line", if all pairs of estimated and observed points lie entirely on this line, then the estimates are perfect.

The three types of 6–hour rainfall estimates data from HMW, NOW and MKV are all positively correlated with the 6–hours observed rainfall. MVK has the strongest correlation, $Corr_{MVK}$= 0.45. HMW and NOW have similar correlation coefficient values with observed rain, while NOW was slightly better as $Corr_{HMW}$ = 0.35 and $Corr_{NOW}$ = 0.36. The ME value of HMW is positive and large (ME_{HMW} = 1.34). Conversely, the 6–hour rainfall estimates from NOW and MVK are lower than the actual measured rainfall as ME_{NOW}=–0.39 and ME_{MVK} =–0.35. This can also be seen through the linear regression lines for MVK and NOW are below the ideal regression line (Figures 2–3). In contrast, the linear regression line of HMW is above the ideal regression line.

Average error magnitude of three data types HMW, NOW and MVK are shown through RMSE values. Error magnitude of HMW is the biggest, $RMSE_{HMW}$ is 19.77. This value is 3.8 times greater than $RMSE_{NOW}$ ($RMSE_{NOW}$ = 5.16) and 4.0 times greater than $RMSE_{MVK}$ ($RMSE_{MVK}$ = 4.93).

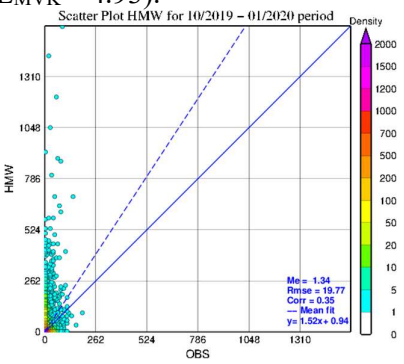

(a)

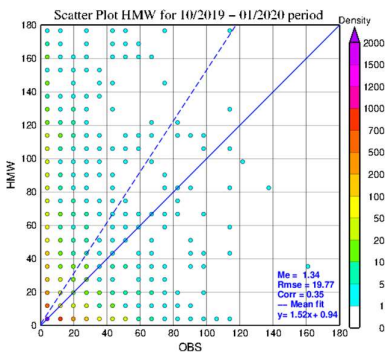

(b)

Figure 2. (**a)** Scatter plot diagram of 6–hour rain gauge observations and Himawari–8 6–hour rainfall estimates; (**b**) Same as in a) but enlarged view for the precipitation range 1–180 mm/6h.

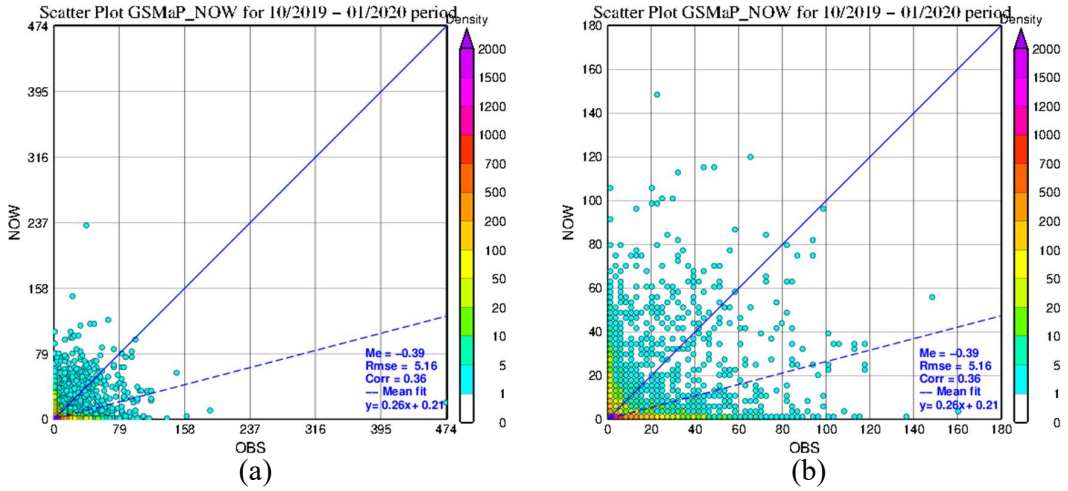

Figure 3. Same as Figure 2 except for GSMaP_NOW.

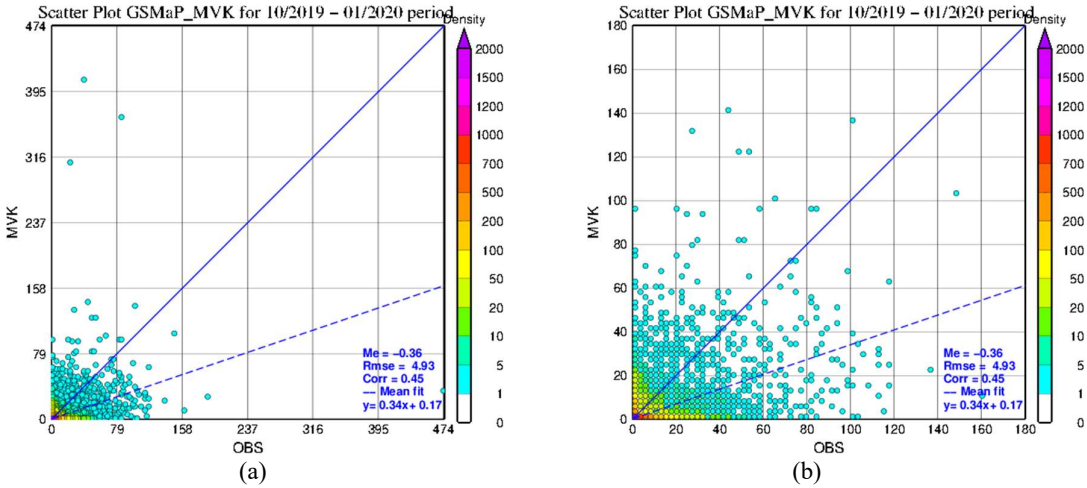

Figure 4. Same as Figure 2 except for GSMaP_MVK.

3.2. Categorical Statistical verifications

Details of the values of TS, POD, FAR, ETS and BIAS indices are shown in Figures.5a, 5b,5c, 5d, and 5e with the event numbers of the contingency table (Table 4). As shown in Figure 5, TS_{HMW}, TS_{NOW}, TS_{MVK} tend to decrease with increasing rainfall thresholds. At all 06h accumulated rainfalls, the values of TS_{MVK} (green) are larger than those of TS_{NOW}(red) and TS_{HMW}(orange).

Table 4. Contingency table by each threshold.

		Hits (FO)	**False alarms (FX)**	**Misses (XO)**	**Correct negative (XX)**	**BIAS**	**POD**	**FAR**	**TS**	**ETS**
	HMW	2170	3152	4772	73243	0.767	0.313	0.592	0.215	0.179
1mm/06h	NOW	1846	1330	5785	79670	0.416	0.242	0.419	0.206	0.181
	MVK	2384	1305	4645	75729	0.525	0.339	0.354	0.286	0.259
10mm/06h	HMW	688	1649	1089	79911	1.315	0.387	0.706	0.201	0.189

		Hits (FO)	False alarms (FX)	Misses (XO)	Correct negative (XX)	BIAS	POD	FAR	TS	ETS
	NOW	398	602	1594	86037	0.502	0.2	0.602	0.153	0.146
	MVK	541	482	1312	81728	0.552	0.292	0.471	0.232	0.224
	HMW	366	1257	505	81209	1.863	0.42	0.774	0.172	0.165
20mm/06h	NOW	202	332	788	87309	0.539	0.204	0.622	0.153	0.149
	MVK	226	230	706	82901	0.489	0.242	0.504	0.195	0.191
	HMW	206	1063	274	81794	2.644	0.429	0.838	0.134	0.129
30mm/06h	NOW	104	226	442	87859	0.604	0.191	0.685	0.135	0.132
	MVK	99	150	424	83390	0.476	0.189	0.602	0.147	0.145
	HMW	126	912	175	82124	3.449	0.419	0.879	0.104	0.101
40mm/06h	NOW	52	155	282	88142	0.62	0.156	0.749	0.106	0.105
	MVK	49	84	270	83660	0.417	0.154	0.632	0.122	0.12
	HMW	81	789	105	82362	4.677	0.435	0.907	0.083	0.081
50mm/06h	NOW	23	101	189	88318	0.585	0.108	0.815	0.073	0.073
	MVK	23	42	176	83822	0.327	0.116	0.646	0.095	0.095
	HMW	50	698	66	82523	6.448	0.431	0.933	0.061	0.06
60mm/06h	NOW	11	60	120	88440	0.542	0.084	0.845	0.058	0.057
	MVK	12	29	111	83911	0.333	0.098	0.707	0.079	0.079
	HMW	37	607	43	82650	8.05	0.463	0.943	0.054	0.053
70mm/06h	NOW	6	33	82	88510	0.443	0.068	0.846	0.05	0.049
	MVK	7	20	78	83958	0.318	0.082	0.741	0.067	0.066
	HMW	25	537	30	82745	10.218	0.455	0.956	0.042	0.042
80mm/06h	NOW	3	19	58	88551	0.361	0.049	0.864	0.037	0.037
	MVK	5	16	53	83989	0.362	0.086	0.762	0.068	0.067
	HMW	14	493	19	82811	15.364	0.424	0.972	0.027	0.026
90mm/06h	NOW	1	14	36	88580	0.405	0.027	0.933	0.02	0.019
	MVK	2	16	34	84011	0.5	0.056	0.889	0.038	0.038
	HMW	6	457	14	82860	23.15	0.3	0.987	0.013	0.012
100mm/06h	NOW	0	10	23	88598	0.435	0	1	0	0
	MVK	2	8	20	84033	0.455	0.091	0.8	0.067	0.067

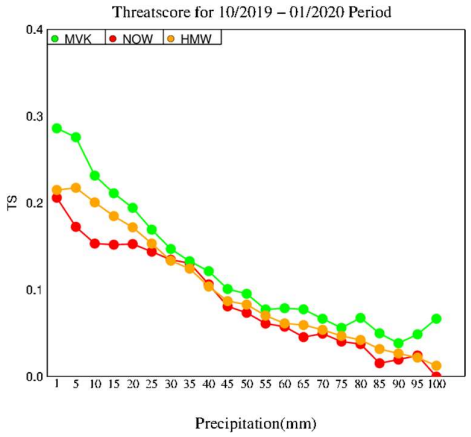

(a)

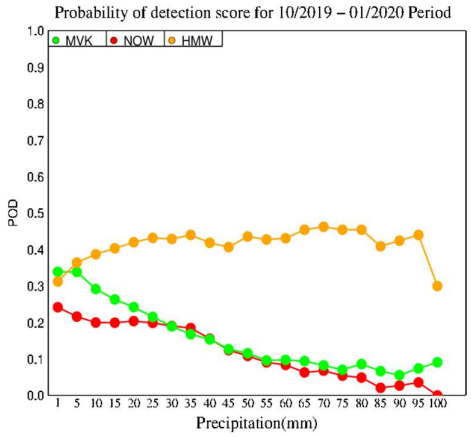

(b)

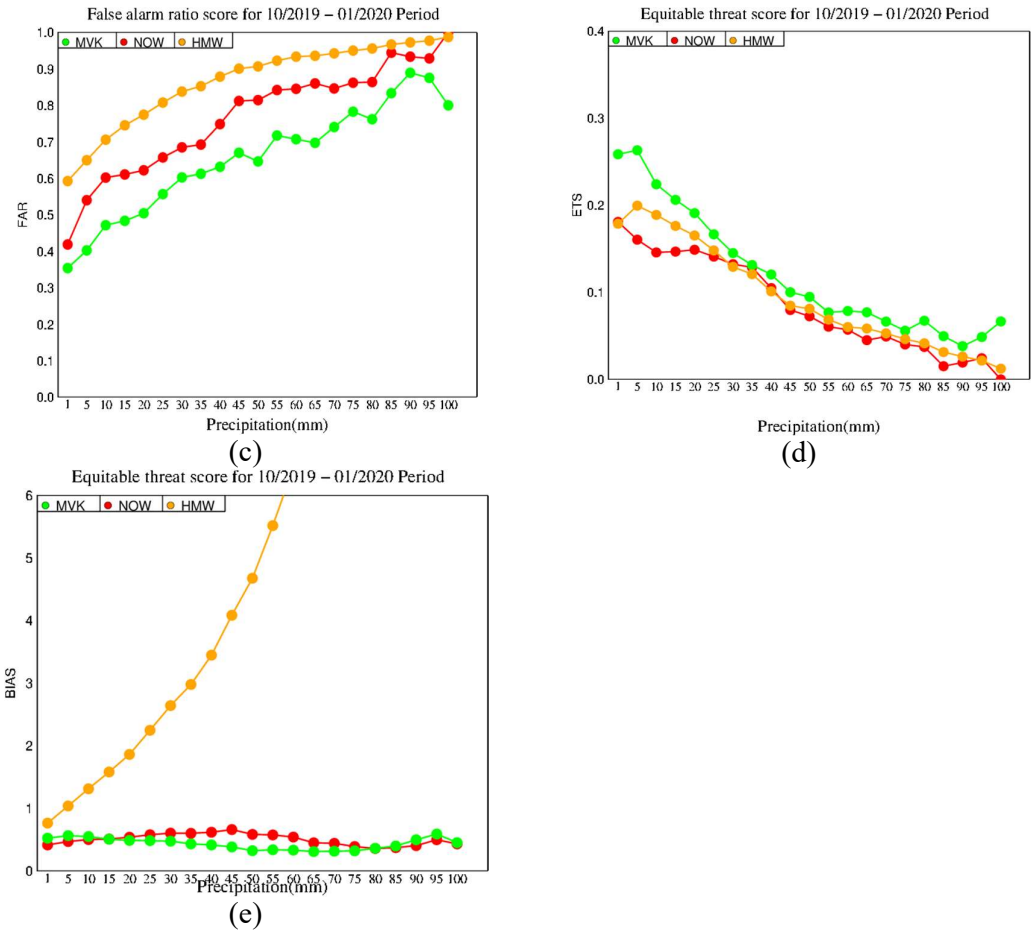

Figure 5. (**a**) Threat scores (TS); (**b**) Probability of detection (POD); (**c**) False alarm rate (FAR); (**d**) Equitable threat score (ETS); (**e**) BIAS of GSMaP_MVK (MVK; green), GSMaP_NOW (NOW; red) and Himawari–8 (HMW; orange).

The values of TS_{HMW} are close to TS_{NOW} but slightly larger than TS_{NOW} at most thresholds except for 30 to 40 mm/06h thresholds. Figure 6 shows POD. POD_{HMW} is larger than POD_{NOW} and POD_{MVK} at most thresholds except for 1 mm/6h. POD of MVK is larger than NOW except for 30 and 40 mm/6h thresholds. When precipitation is overestimated, the value of POD tends to be large, but it does not mean that the estimate is good. Therefore, POD should be checked with FAR. As seen in Figure 5c, FAR_{HMW} is the largest for thresholds from 1 to 95 mm/6h. This is consistent with the results on ME_{HMW} and $RMSE_{HMW}$ where ME_{HMW} is positive and $RMSE_{HMW}$ is the largest (19.77 mm).

In FAR (Figure 5c), FAR_{HMW} (orange) is always the largest except for 100 mm/6h threshold, suggesting its overestimation of rains. NOW has the second largest false alarm, and the red line is between the green and orange lines. FAR_{MVK} is the smallest at all thresholds. The overall trend of ETS_{MVK}, ETS_{NOW} and ETS_{HMW} (Figure 5d) is like those of TS (Figure 5a), as ETS_{MVK} is the largest at all thresholds, and the values of ETS_{HMW} and ETS_{NOW} are similar. The relationship between the ETS_{HMW} and ETS_{NOW} is also almost the same as in TS, but at the threshold of 01 mm/06h ETS_{NOW} is larger than ETS_{HMW}, and around 30 to 40 mm/06h superiority of ETS_{NOW} against ETS_{HMW} is more distinct in ETS (Table 4). Generally, ETS has a merit to offset the false gain by overestimation in TS, but in our case, the merit was not large due to the smallness of hit_{random} (Eq. 9). Calculation results of BIAS values of NOW, MVK and HMW are shown in Figure.5e. The $BIAS_{NOW}$ and $BIAS_{MVK}$ are less than 1 at all rainfall thresholds. This is consistent with ME_{NOW} and ME_{MVK}. In contrast,

$BIAS_{HMW}$ is less than 1 at only 01 mm/06h threshold then increases rapidly with rainfall thresholds. $BIAS_{HMW}$ is extremely large for intense rains as shown in Table 4 (e.g., 24 at 100 mm/06h threshold).

Here we show an example of rainfall overestimation by HMW on October 7–8, 2019 in Thai Binh province, the northeast coastal area of Vietnam. Thai Binh Rain gauge station has coordinates of 20.4ºN and 106.4ºE (Table 2). At the station location, HMW 6–hour rainfall estimation from 18 UTC 07 October 2019 to 00UTC 08 October 2019 was 324.6 mm. This value is 12 times larger than the actual observed value (27 mm). Estimated rainfall from MVK and NOW are 46.8 mm and 54.2 mm, respectively (Figure 6).

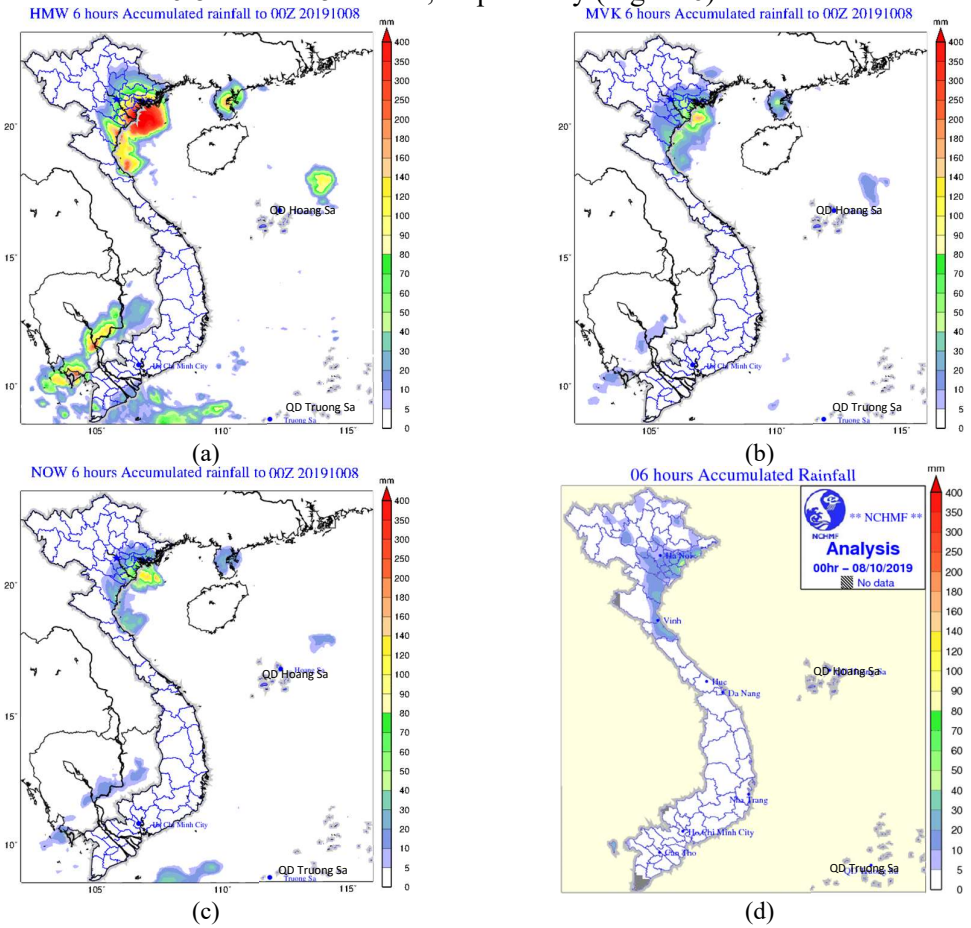

Figure 6. Six–hour estimated rainfall from 18 UTC 07 October 2019 to 00 UTC 08 October 2019: (a) Himawari–8; (b) GSMaP_MVK; (c) GSMaP_NOW; (d) SYNOP rain gauges.

Figure 7 is Himawari–8 IR images at 19 UTC 7 October 2019, and Figure 9 indicates the time sequence of the brightness temperatures (T_{BB}) around Thai Binh station and corresponding rainfall estimates by Himawari-8 (HMW). T_{BB} around Thai Binh at 19 and 20 UTC were –75.3 ºC and –70.1 ºC, respectively, and in these two times HMW recorded the largest values as 70.75 mm/h and 85.96 mm/h. As discussed in [5], to give rainfall estimation from Himawari–8, AMO uses relationship between T_{BB} and rainfall intensity R:

$$R = 1.1183*10^{11} exp(-3.6382*10^{-2} T_{BB}^{1.2}) \quad (11)$$

This relationship (Figure 8) is based on statistics between T_{BB} observed by GOES satellite and radar–estimated rainfall over north America [4].

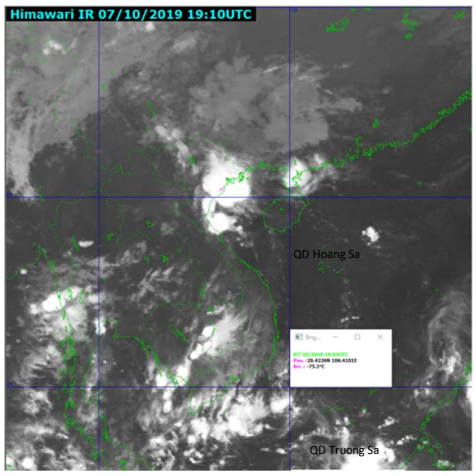

Figure 7. Infrared image by geostationary satellite (Himawari–8) at 19z 7 October 2019.

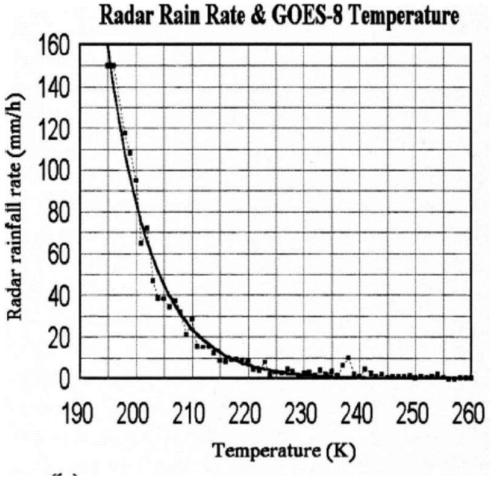

Figure 8. Relationship between TBB and rainfall rate [4].

Figure 9. Horizontal distribution of Himawari–8 6–hour precipitation estimate at Thai Binh station.

Figure 10 is the time variation of 06 hours accumulated rainfall from NOW (red line), MVK (green line), HMW (orange line) and 06h rain gauge (black line) in 5 heavy rainfalls in Vietnam from October 2019 to the end of January 2020. In general, the rainfall estimated from NOW, MVK and HMW show precipitation changes. The shapes of yellow, red, orange

lines are quite like black line. However, specifically in each rain, rainfall estimates from NOW, MVK and HMW also have differences.

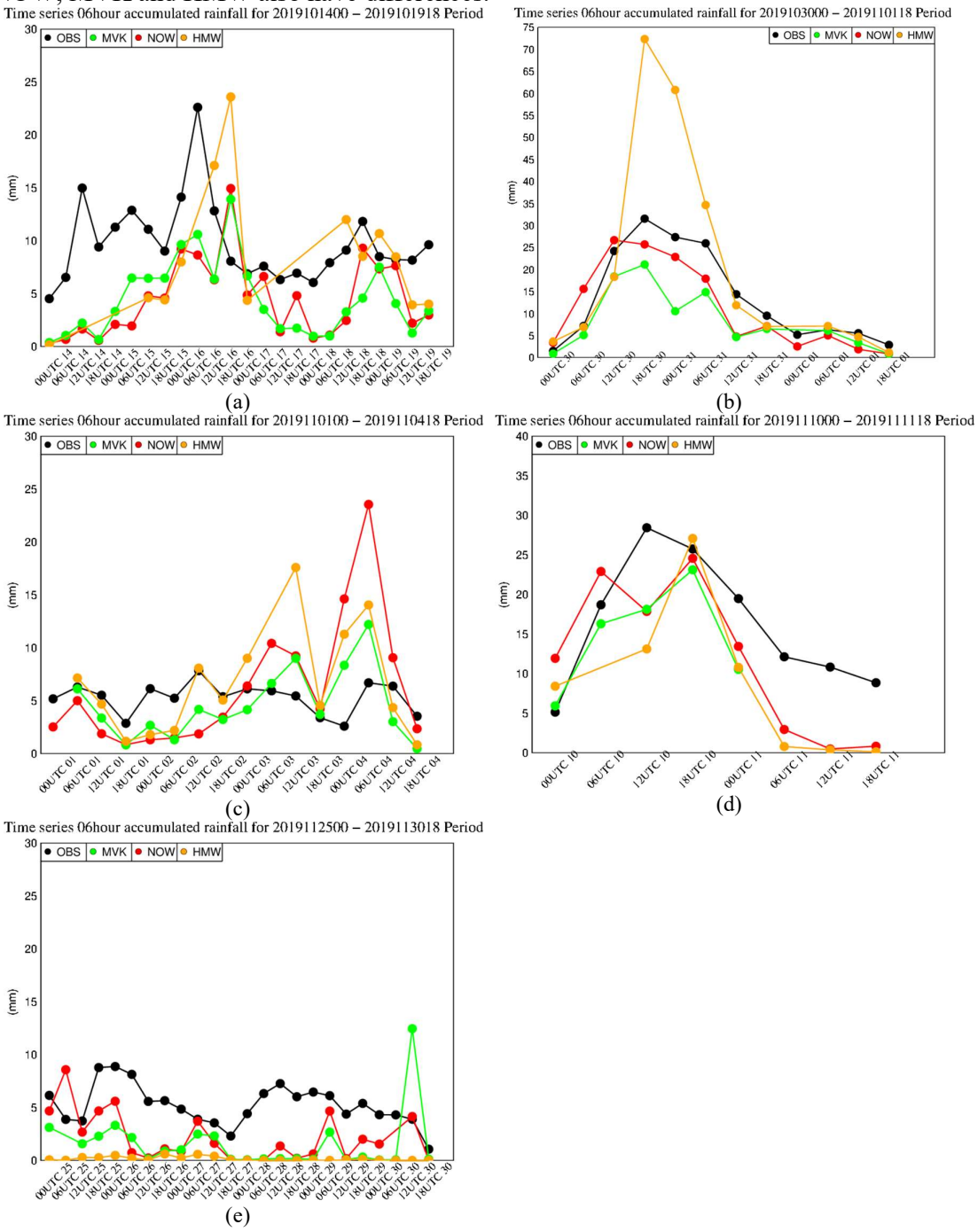

Figure 10. variation of 06 hours accumulated rainfall from NOW (red line), MVK (green line), HMW (orange line) and 06h rain gauge (black line) in 5 heavy rainfalls in Vietnam from October 2019 to the end of January 2020.

From 14th to 19th Oct (Figure 10a), rainfall estimated from NOW and MVK tend to be lower than observed. The black line is above the red line and the blue line. The rainfall estimated from HMW is higher than NOW and MVK and quite like the observed. From 30th Oct to 01st Nov (Figure 10b), rainfall estimated from NOW, MVK showed the variation of rainfall. Rainfall increased gradually and peaked during the 12UTC 30th to 00UTC on 31st

October period, then it dropped. Estimation of rain from HMW also shows this trend, however, the maximum rainfall of HMW is too large compared to the observed. Maximum value of HMW is 73mm. In fact, the maximum of rain gauge is just over 30mm. From 01st to 04th Nov (Figure 10c), before 12UTC 02nd NOV, the rainfall estimates from NOW, MVK and HMW all tended to be lower than rain gauge. After this point of time, the precipitation estimated from them tend to overestimate the rainfall which observed. From 12UTC 02nd Nov to 12UTC 03rd Nov, HMW gave the highest rainfall estimate. NOW has the highest rainfall estimate in the remaining period. Figure 10d shows the NOW, MVK, HMW estimated rainfall reflect actual precipitation patterns. The rainfall increased and decreased rapidly before and after the 06UTC–12UTC 10th Nov. However, the rainfall estimates are lower than reality. The most obvious low rainfall estimations occurred from 00UTC to 18UTC 25th Nov (Figure 10e). Most of the time, the 06h accumulated rainfall estimations are smaller than observed. In particular, the rainfall from the HMW is very small during this rain period.

4. Summary and concluding remarks

This study verified the quality of three rainfall estimates by GSMaP_NOW, GSMaP_MVK and Himawari–8 against 6–hour rain gauge data from 184 SYNOP stations for a 4–month period from October 2019 to January 2020. The three types of data were positively correlated with the observed rainfall. In particular, GSMaP_MVK has the highest correlation. The rainfall estimated from Himawari–8 was excessive compared with the actual data and has the largest RMSE. GSMaP_NOW and GSMaP_MVK rainfall estimates were slightly lower than actual ones. The RMSE of GSMaP_MVK was the smallest among the three estimates. GSMaP_MVK has the best rainfall estimation skills of the three data types in FAR, TS and ETS in all thresholds. TS_{HMW} was slightly larger than TS_{NOW} except from 30to 40mm/6h thresholds. POD_{HMW} was the largest, but this is derived from HWM's excessive rainfall estimates, because FAR_{HMW} value was the largest. The POD_{MVK} was larger than POD_{NOW} and the FAR_{MVK} was smaller than FAR_{NOW}.

The excessive rainfall estimates by Himawari–8 seen in this study is very different from the results in Saito et al. (2020) [5], which verified the three rainfall estimates against AWS 3–h rains for the case of the Da Nang heavy rainfall event in December 2018. Targeted rainfall in Saito et al. (2020) [5] was mainly brought by a precipitation system whose cloud top was not high, and warm rain process was likely dominant. In the Da Nang heavy rainfall event, Himawari–8 drastically underestimated intense rains. Contrary, Himawari–8 tends to overestimate intense rains if could top brightness temperature is extremely low. Such the cases easily occur not only by deep convection but by dense cirrus and anvil overcast.

In conclusion, GSMaP_MVKwasthe best rainfall estimate amongthe three data, but due to a delay of 3–4 days, it is not applicable to the operational forecasting and warning. Consequently, itis recommended to use GSMaP_MVK mainly for verification of NWP rainfall. GSMaP_NOW has a relatively good rainfall estimate, which can be used in parallel with Himawari–8 rainfall estimates to provide realtime information to the forecasters in forecasting and warning on the heavy rainfall, flash flood andlandslide.

Author Contributions: Author Contributions: Conceptualization, M.K. Hung; methodology, M.K. Hung, K. Saito, and D.D. Tien; validation, M.K. Hung, D.D. Tien; Rain gauge data curation, M.K. Hung, Satellite data curation, N.V. Hung, M.K. Hung, writing–original draft preparation, M.K. Hung; writing–review and editing, M.K. Hung, K. Saito, M.V. Khiem, D.D. Tien; supervision, K. Saito; All authors have read and agreed to the published version of the manuscript.

Funding: This study was supported by a project from the Ministry of Agriculture and Rural Development: “A study to forecast flood situation on Bac Nam Ha irrigation system to

support decision making of drainage pumps water in real time" coordinated implementation between the Institute of Water Resources Planning and the National Center for Hydro–Meteorological Forecasting.

Acknowledgments: We would like to thank Project of the Ministry of Agriculture and Rural Development: "A study to forecast flood situation on Bac Nam Ha irrigation system to support decision making of drainage pumps water in real time" for financial supports. We also thank AMO for satellite estimated rainfall data and JAXA on GSMaP data.

Conflicts of Interest: The authors declare no conflict of interest.

References

1. Eckstein, D.; Hutfils M.L.; Winges, M. Global Climate Risk Index. **2019**. Available online: https://germanwatch.org/files/Global%20Climate%20Risk%20Index%202019_2.pdf
2. Artan, G. Adequacy of satellite derived rainfall data for stream. *Nat. Hazard* **2007**, *43*, 167–185.
3. Hossain, F.; Katiyar, N.; Hong, Y.; Wolf, A. The emerging role of satellite rainfall data in improving the hydro–political situation of flood monitoring in the under–developed regions of the world. *Nat. Hazards* **2007**, *43*, 199 – 210.
4. Vicente, G.R.; Scofield, A.; Mensel, W.P. The operational GOES infrared rainfall estimation technique. Bull. *Amer. Meteor. Soc*. **1998**, *79*, 1881–1898.
5. Saito, K.; Hung, M.K.; Hung, N.V.; Vinh, N.Q.; Tien, D.D. Heavy rainfall in central Viet Nam in December 2018 and modification of precipitation nowcasting at VNMHA. *VN J. Hydrometeorol.* **2020**, *5*, 65–79.
6. Kim, H.; Kubota, T.; Utsumi, N.; Ishitsuka, Y.; Yoshimura, K.; Oki, R.; Oki, T. Development and Applications of the GSMaP: Overview & Lessons learned in a real–world case for Hydrological Status and Outlook System. 2017. Available online: http://www.wmo.int/pages/prog/hwrp/chy/hydrosos/documents/presentations/day2/Session3–Hyungjun_Kim–GSMaP.pdf
7. Hieu, B.T.; Ishidaira, H.; Shaowei, N. Evaluation of the use of global satellite–gauge and satellite only precipitation products in stream flow simulations. *Appl. Water Sci.* **2019**, *9,* 53.
8. Thanh, N.D.; Matsumoto, J.; Kamimera, H.; Hai, B. Monthly adjustment of Global Satellite Mapping of Precipitation (GSMaP) data over the Vu Gia–Thu Bon River Basin in Central Vietnam using an artificial neural network. *Hydrol. Res. Lett*. **2013**, *7*, 85–90.
9. Joyce, R,J.; Janowiak, J.E.; Arkin, P.A.; Xie, P.P. Cmorph: a method that produces global precipitation estimates from passive microwave and infrared data at high spatial and temporal resolution. *VN J. Hydrometeorol.* **2004**, *5*, 487–503.
10. Ushio, T.; Kubota, T.; Shige, S.; Okamoto, K.; Aonashi, K.; Inoue, T.; Takahashi, N.; Iguchi, T.; Kachi, M.; Oki, R.; Morimoto, T.; Kawasaki, Z. A Kalman filter approach to the Global Satellite Mapping of Precipitation (GSMaP) from combined passive microwave and infrared radiometric data. *J. Meteor. Soc. Japan* **2009**, *87A*, 137–151.
11. Kachi, M.; Aonashi, K.; Kubota, T.; Shige, S.; Ushio, T.; Mega, T.; Yamamoto, M.; Hamada, A.; Seto, S.; Takayabu, Y. N.; Oki, R. Developments and applications of

the Global Satellite Mapping of Precipitation (GSMaP) for the Global Precipitation Measurement (GPM). *Geophys. Res. Abstracts* **2016**, *18*, EGU2016–11384–1.

12. Oki, R. GSMaP and its applications. 2017. Available online: http://www.wmo.int/pages/prog/sat/meetings/workshop_on_SWCEM/documents/7(1)_20160216_WMO%20WS_JAXA.pdf
13. Takeuchi. Outline of operational numerical weather prediction at the Japan Meteorological agency. 2013. Available online: http:// https://www.jma.go.jp/jma/jma–eng/jma–center/nwp/outline2013–nwp/index.htm